Journal of Materials Chemistry A

Accepted Manuscript

ROYAL SOCIETY OF CHEMISTRY

www.rsc.org/materialsA

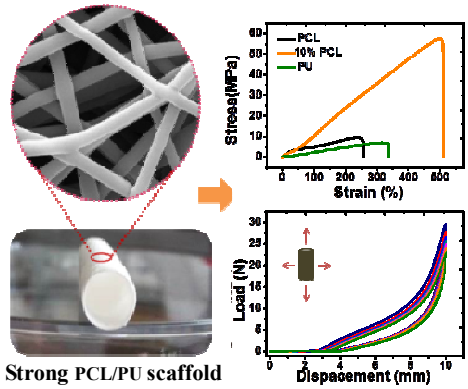

A high-strength PCL/PU composite vascular with excellent cycle stability and cell compatibility were fabricated by electrospinning.

Journal of Materials Chemistry A RSCPublishing

COMMUNICATION

Electrospun Strong PCL/PU Composite Vascular Graft with Mechanical Anisotropy and Cyclic Stability

Cite this: DOI: 10.1039/xoxxoooooox

Fengyun Guo,[a] Nü Wang,*[a] Li Wang,[b] Lanlan Hou,[a] Lan Ma,[a] Jing Liu,[a] Yuee Chen,[a] Bingbing Fan,[a] and Yong Zhao*[a]

Received ooth January 2012,
Accepted ooth January 2012

DOI: 10.1039/xoxxoooooox

www.rsc.org/

A strong PCL/PU vascular graft was fabricated using electrospinning. By regulating the content of PCL, the composite scaffolds show obvious mechanical enhancement with strength up to 69.95 MPa. Furthermore, the scaffolds exhibit high porosity, mechanical anisotropy, cell compatibility and cycle performance, which are important for tissue engineer applications.

Vascular disease is a serious threat to the health of people.[1] Thus, there is an urgent demand for high-performance vascular graft. Artificial vascular scaffold is a kind of tube that serves as replacements for damaged or injured blood vessels. As a functional construct, it is essential that an engineered vascular graft should meet certain basic criteria, such as biocompatibility for cell proliferation and growth, porosity favorable of diffusion for the nutrients and waste, and so on.[2] But for practical application, what should be first taken into account is the mechanical property of the graft including adequate strength, elasticity and mechanical durability to withstand puncture and cyclic loading. Over the past several years, substantial progress has been made in designing materials with excellent mechanical properties using diverse materials [3,4] and methods such as ice templating,[5] doping,[6] vacuum filtration.[7] Despite the stirring and exciting progress, most of the aforementioned materials and methods will be unavoidably confronted with cost, bioactivity or cyclic elasticity issues in terms of practical applications in tissue engineering of vascular grafts.

Currently, the available options for these vascular graft transplants are autologous grafts, allografts, xenografts, artificial prostheses and synthetic vascular grafts made of expanded polytetrafluroethylene (ePTFE) and polyethylene terephthalate.[8] Regrettably, by using these available options, a series of problems including unsuitable diameter, mechanical compliance and construction occurred after a certain period. In order to obtain artificial blood vessels suitable for transplantation, a number of methods were explored and developed, such as molecular self-assembly, hydrogels, thermally induced phase separation.[9] The utilization of these methods and materials brings significant results for preparation of vascular grafts. However, further improvement and optimization were still needed since the aforementioned methods are not optimal in terms of practical application. The main problems of the failure could be ascribed to the lack of control for mechanical property, composition, vascular dimension and morphology. Thus, developing a suitable method to prepare the available artificial blood vessels is particularly necessary.

Electrospinning,[10] which can flexibly tune the structure,[11,12] composition[13] and performance[14-16] of scaffolds and optimize cell adhesion as well as guide their behaviour,[17] is an effective method to prepare scaffolds for tissue engineering.[18-20] For example, a bilayered scaffold was prepared using electrospinning based on PCL and collagen and endothelial cells (EC) adhesion and smooth muscle cells (SMC) infiltration were studied.[21] Also, a modified approach, electrospray concurrently with the electrospinning in order to obtain nanofibrous scaffolds of rough surface for cell attachment and proliferation, has been developed.[22] Recently, several materials,

[a]*Key Laboratory of Bioinspired Smart Interfacial Science and Technology of Ministry of Education, Beijing Key Laboratory of Bioinspired Energy Materials and Devices, School of Chemistry and Environment, Beihang University, Beijing 100191, China. Fax:+86-10-82317801; Email: wangn@buaa.edu.cn; zhaoyong@buaa.edu.cn*

[b]*Beijing National Laboratory for Molecular Sciences (BNLMS), Key Laboratory of Organic Solids, Institute of Chemistry, Chinese Academy of Sciences, Beijing, 100190, China.*

† Electronic Supplementary Information (ESI) available: [details of any supplementary information available should be included here]. See DOI: 10.1039/c000000x/

including PVDF-HFP,[23] PGS/PCL,[24] PLLA/PDMS,[25] have been used in preparation of artificial vascular graft. In these reports, uniaxial mechanical property and biocompatibility were often mentioned. However, some particular mechanical properties should not be neglected because reported materials or properties are not strong enough to satisfy the requirement of practical applications, for example, i) most of the mechanical properties are often reported in terms of uniaxial tensile (almost all in longitudinal direction), it cannot represent the comprehensive mechanical performance, by contrast, lateral tension properties are more important for clinical success of blood vessels; ii) the cycle performance, which is crucial to display material flexibility, pliability and mechanical durability, are poorly discussed; iii) for specific applications, such as saphenous vein (long, σ = 13 MPa),[26] the strength of current materials are still weak.

Polyurethane (PU), an elastic polymer and consisting of soft and hard segments, is a biocompatible materials. Polycaprolactone (PCL), a viscous and nontoxic polymer, is an ideal reinforcer due to its semi-crystallization and functional group similar to PU. Both of them, characterized by its good biodegradability and biocompatibility, are widely used in the design of biomaterials,[27,28] which make them desirable building blocks for assembling vascular scaffolds. Compound formed by two or more materials in certain ways can play advantages of each materials, show performances that single material does not have and expand the applications of integrated materials. With this inspiration, here we developed a biocompatible PCL/PU composite with excellent mechanical properties, where the strength and elongation of composite demonstrated significant improvement (over 800% for strength enhancement) compared to pure PU. Subsequently, small diameter artificial PCL/PU composite vascular scaffolds were fabricated using electrospinning and pulling-out method, of which the overall porosity, biaxial tensile mechanical properties, cyclic mechanical durability and cell compatibility were examined. The results indicated that PCL could substantially enhance the strength of the PU and PCL/PU composite tube could be a promising candidate for small diameter vascular graft.

In this work, PCL/PU composite fibrous film and small diameter vascular grafts were fabricated by electrospinning. With appropriate ratio, the mechanical properties of the composite get obvious improvement compared with pure PCL or PU. Fig 1 shows the typical SEM images and diameter distributions of as-prepared films. The top of the Fig 1a-1d are images of pure PU, PCL/PU (10% PCL), PCL/PU (25% PCL) and pure PCL nanofibers, respectively. Displayed in the bottom are corresponding diameter distributions. It is seen that all the resulting fibers intersected closely and oriented randomly. The average diameters of them are about 660 nm, 730 nm, 830 nm and 760 nm, respectively. All samples are of close average fiber diameters and corresponding diameter distributions is narrow, indicating uniform morphology of PCL/PU composite. For each film, the fibers are continuous, uniform, macroscopically smooth and without evident gross defects. In order to optimize mechanical performance, fibers morphology and diameter were regulated and controlled by adjusting the parameters of the electrospinning including voltage, needle diameter, working distance, humidity, solvent and concentration of solutions.

To assess the mechanical properties of those films, tensile experiment was performed at room temperature (25 ℃) with a loading rate of 10 mm/min. Fig 2a shows uniaxial stress–strain curves of films under tensile loading. All films show a nearly short

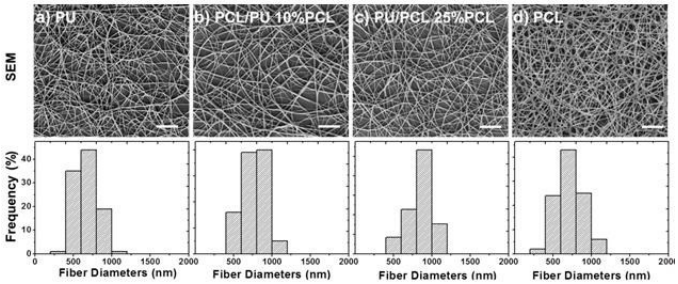

Fig. 1 Representative SEM images and diameter distributions of as-prepared electrospinning fiber films: a) pure PU, b) PCL/PU with PCL content of 10%, c) 25%, d) pure PCL. All the fibers, with relatively smooth surfaces, are continuous and randomly oriented. In an effort to optimize mechanical performance, films morphology was regulated and controlled by adjusting the parameters of the electrospinning, relative proportions of mixed solvent and concentration of solutions. The bottom of the Fig show the diameters distribution of the fibers, and the average diameter are 660 nm, 730 nm, 830 nm and 760 nm, respectively. The fiber diameter distributions were generated from SEM images by Image J software. Scale bar = 20 μm.

linear region with a relatively steeper slope in the initial stress–strain curve followed by a long linear region. However, the breaking strength, modulus and elongation of pure PU and PCL/PU are significantly different. The tensile strength and elongation of the pure PU films are 7.84 ± 1.25 MPa and 355.67 ± 16.48%, which are similar to the previously reported values.[29] With the addition of PCL, the tensile stress increases firstly and then decreases after reaching a certain threshold. Fig 2b shows statistical graph of strength for PCL/PU composite in different ratios. From Fig 2b, we could obviously see that the composite with the PCL content of 10% has the strongest tensile strength of 60.45 ± 8.01 MPa, which is more than eight times of the pure PU film. Fig 2c and 2d are modulus and elongation of the composite. The maximum value of elongation can even reach 512.32%, which indicated good pliability and flexibility of the PCL/PU films. It revealed that adding a certain amount of PCL to PU, the mechanical properties of the composite can be greatly improved. Furthermore, with the PCL contents of 10% and 25%, the strength and toughness of the composites show synergistic enhancement (orange and green curve shown in Fig 2a). These results demonstrate that PCL plays a notable role in improving the strength of PU without sacrificing the elasticity of composite. It is supposed that there are three reasons that can account for this phenomenon: i) PCL, a semicrystalline polymer, possess of many characteristics including good viscoelasticity, biocompatibility and functional group which is the same as PU (Fig S1). With the addition of a certain amount of PCL, the solution of PCL and PU showed good compatibility in mixed solvent. And the DSC (Fig S2) results showed that the degree of crystallinity[30,31] for composite films also increased with a certain amount of PCL adding, as reflected by the increased melting point; ii) the electrospinning PCL/PU composite films have a high densification, which is result from the bonding, interconnecting[32-34] and intersection between the fibers, as shown in Fig S3, these bonding points and entanglement hinder the fibers slipping in the process of tensile, giving rise to load transfer; iii) the addition of PCL to PU increases the rigid component content thereby increasing the strength and supramolecular structure was formed. With further increasing PCL content, joints decreased and phase separate were occur in the composite material.[35-37]

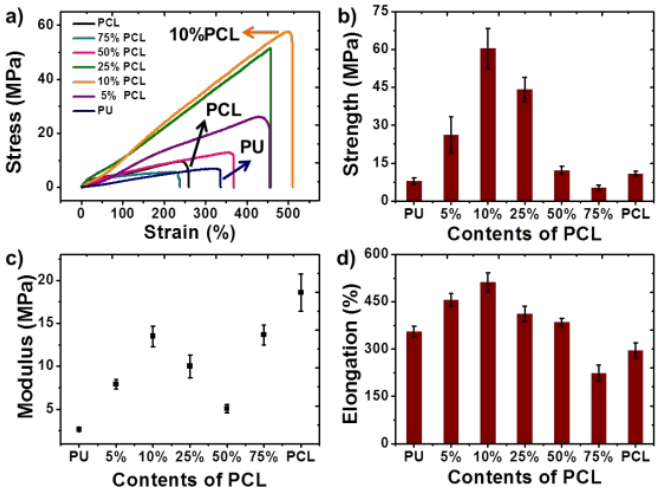

Fig. 2 Typical mechanical properties of pure and composite PCL/PU fibrous films. a) Representative tensile stress-strain curves, b) ultimate tensile strength, c) modulus and d) elongation of pure and composite fiber films. All the films were measured at room temperature with a speed of 10 mm/min. The mechanical properties of the composite were enhanced considerably compared with pure PU (dark blue), especially for films with PCL contents of 10% (orange) and 25% (green). The maximum strength (60.45 ± 8.01 MPa) is 771% of the pure PU (7.84 ± 1.25 MPa). More importantly, there is a synergetic reinforcement in terms of tensile strength and elongation.

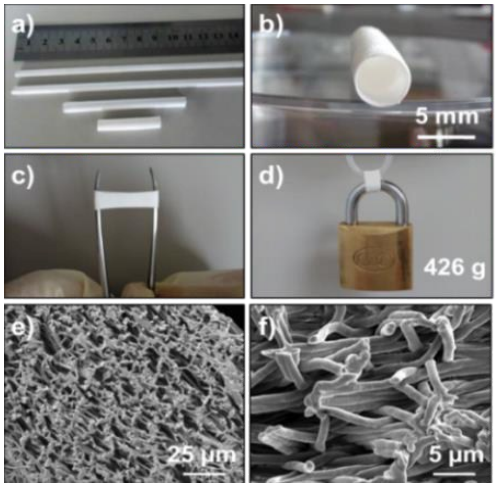

Fig. 3 Digital camera images and scanning electron micrographs of PCL/PU artificial blood vessels. a) Whole appearance of artificial blood vessels having different lengths and diameters produced. b) side view of the typical tubular scaffold with an diameter about 5 mm and a length of 6 cm, c) a round tube was stretched to flat shape using tweezers. d) Photograph showing a 426 g weight hanging on a segment with about 5 mm diameter and 4 mm length. After five minutes, the segment is still intact. Fig 3c and 3d demonstrated good flexibility, pliancy and strength of the tube. e), f) cross-sectional view with different magnifications showing intersection, stack and bonding of the fibers. The resulting fibers are uniform and oriented randomly. There is no significant change for the morphology of scaffolds after immersed in water.

Based on outstanding mechanical properties of the PCL/PU, several vascular grafts were fabricated using electrospinning. Here, the composite with PCL content of 25% was used as typical example for fabrication of vascular grafts in consideration of mechanical properties and fiber porosity. Fig 3 are the morphology of as-prepared vascular scaffolds. The precursor solution is the same as the corresponding fibrous films. And stainless steel and hollow mandrels with a rotating speed of 60 r/min connected with motors were used to fabricate the tubular-shaped construct (Fig S4). As shown in Fig 3a, tubes with different diameter and length were prepared using electrospinning and pulling-out method. A typical PCL/PU tubular scaffold, having a diameter about 5 mm and a length of 6 cm was displayed in Fig 3b. Then segments cutting from as-prepared tubular scaffold were conducted for a period of time to testify the mechanical property.As shown in Fig 3c, a round tube was stretched to flat shape using tweezers, which indicated good pliability of the tube. Fig 3d is a photograph showing a 426 g weight object hanging on a tube segment with 5 mm diameter and 4 mm length. After five minutes, the tube segment is still intact. Fig 3e and 3f are cross-sectional SEM images of the tube at different magnifications. The resulting fibers are uniform and oriented randomly. Intersecting and bonding of the fibers in tube is obvious (Fig 3f). Apart from morphology and structure, the overall porosity of the PCL/PU (PCL of 25%) tube was estimated using following equation,[38]

$$\varepsilon = \left(1 - \rho / \rho_o\right) \times 100\%$$

$$\rho = m / V$$

$$\rho_o = \left(x + y\right) / \left(x / \rho_{PCL} + y / \rho_{PU}\right)$$

where ε is the porosity; ρ is the density of the samples calculated from volume $(V = lwh)$ and dry weight (m) of the tubular scaffold; l, w and h represents the length, width and height of the rectangular sheet cutting from as-prepared fiber tube; $x : y$ is the mass ratio of component in the composite; ρ_o is derived from the standard density of PCL (1.145 g/mL) and PU (1.176 g/mL). The calculated overall porosity reached 70.55 ± 3.24%, which was in favor of cellular infiltration and diffusion for metabolites, nutrients and waste.

Mechanical anisotropy and cycle performance are very important for the elastic expansion and retraction of blood vessels in tissue engineer applications. Fig 4 are typical tensile mechanical properties of tube in different directions. A gauge length of 5 mm other tensile test parameters are the same as fiber films. And the results of stress-strain curves were also calculated from load-displacement curves. It is noteworthy that tubes in different directions exhibited significant anisotropy in mechanical properties. Fig 4a displayed the typical stress-strain curve for longitudinal tensile of the PCL/PU tube. The maximum strength is about 69.95 MPa, which is higher than homologous fiber film. However, the elongation decreases from about 465% to 255%. It can be explained by the intersecting and stacking between the fibers observed in vascular graft, as summarized in Fig S5. For lateral tensile (Fig 4d), the maximum strength is 42.5 MPa. The mechanical anisotropy (in different tensile direction) was mainly attributed to the structure and morphology of the fiber tube. In brief, the process of tube formation by means of rotating mandrel is the formation of continuous and closed 3D network fiber architecture. In the process of longitudinal tensile, the continuous and closed 3D network structure is

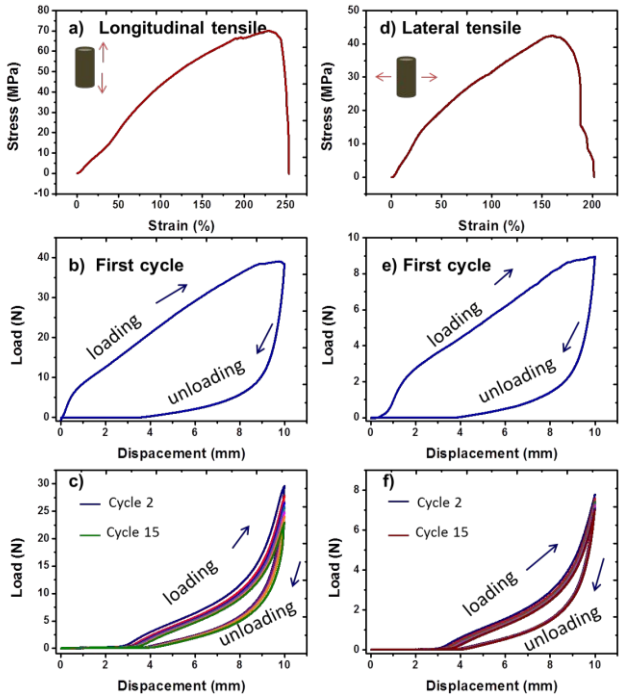

Fig. 4 Biaxial tensile mechanical properties and elastic recovery behavior during cyclic stretching of PCL/PU artificial blood vessel. (a-c) Longitudinal stretch. The maximum strength is about 69.95 MPa. (d-f) Lateral tensile. The maximum strength is about 42.5 MPa. This indicated tensile anisotropy of the tube. In cyclic mechanical tests, there is an obvious hysteresis for first cycle curves regardless of tensile direction. From the second cycle to 15 cycles, the tube shows no significant change in the mechanical property.

conducive to suppress and restrain the fiber slippage, which is absent in lateral tensile.

Although vascular grafts are increasingly developed and exploited, their cyclic mechanical stability, determining their practical applications, is seldom investigated and understood. Therefore, besides uniaxial tensile properties, a set of cyclic mechanical tests was carried out in order to understand the dynamic compliance, fatigue behavior and mechanical durability of PCL/PU tubular vessel. The cyclic tensile curves of PCL/PU tube with the strain 200% are shown in Fig 4b, c (longitudinal tensile) and Fig 4e, f (lateral tensile). We can clearly find that the cyclic stress–strain curves of different tensile directions are similar in their shape and the curves of the first cycle (Fig 4b, e) were much broader than the following cycles. In the first cycle, the loading curves show three regions: i) an initial linear region from0 to about 20% with a steep slope; ii) a long, stable and successive linear regionwith the stress rising relatively slowly at strains of 20–170%; iii) the slope of the loading curve showed a break down at the strain of about 170% followed by a gentle increase of stress. In terms of loading and unloading regions, there is an obvious hysteresis in first cycle regardless of tensile direction. This irreversible hysteresis also caused that maximum cyclic stress in the following stress–strain cycles is lower than that of the first cycle. From the second cycle to following, all the curves were nearly overlapped with each other and each of them showed two regions: a quasi-linear region and another one with a steeper slope. And after 15 cycles, the loss for total strain is not evident and the cyclic mechanical properties are still stable. These phenomena show that no breakdown occurred in these tests.

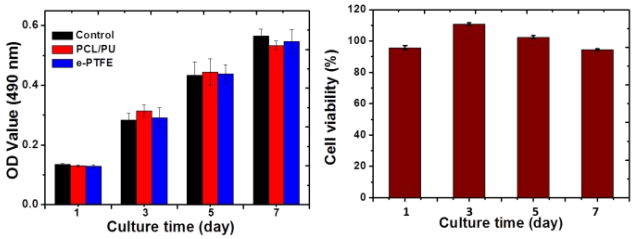

Fig.5 The cytotoxicity (Fig 5a) and cell viability (Fig 5b) of mouse fibroblast cells (L929) on the control, PCL/PU composite and e-PTFE scaffolds in different culture times at 490 nm according to MTT assay. Composite PCL/PU scaffold are found to be non-cytotoxic, with relative cell viability greater than 93%. These results indicated good cytocompatibility of PCL/PU fibrous scaffold. Initial cell density for seeding is 2000 cells/well.

Culture time	Control	PCL/PU	e-PTFE
Day 1	0.136 ± 0.003	0.130 ± 0.003	0.129 ± 0.005
Day 3	0.283 ± 0.024	0.314 ± 0.021	0.292 ± 0.034
Day 5	0.434 ± 0.044	0.444 ± 0.045	0.438 ± 0.031
Day 7	0.565 ± 0.024	0.534 ± 0.016	0.546 ± 0.042

Table 1. MTT assay to evaluate the cytotoxicity (Mean ±SD)

For all the cycle curves, the unloading region including the first cycle were nearly identical, indicating that the energy stored in each cycle was unchanged. These excellent mechanical properties make PCL/PU tube a promising candidate for tissue engineering of vascular grafts.

Being a qualified vascular graft, cytocompatibility is indispensable for the growth and proliferation of the cells in application. Mitochondrial metabolic (MTT) assay, a common method to determine cytotoxicity, was used here for the purpose of testing cell adhesion and viability. Table 1 and Fig 5 shows the proliferation of mouse fibroblast cells (L929) on the negative control, PCL/PU composite and e-PTFE scaffolds in different culture times. Notably, with the culture time increasing, there is an obvious increase for the optical density (OD) values (Fig 5a). And composite PCL/PU scaffold are found to be non-cytotoxic, with relative cell viability greater than 93% (Fig 5b). Another phenomenon should be noted particularly is that the OD values of the as-prepared PCL/PU hybrid scaffold is even higher than negative control and e-PTFE scaffolds at days 3 and 5. These results indicated that the PCL/PU fibrous scaffold is nontoxic on the L929 cells, which proving their potential ability to support cell proliferation and utility for vascular tissue engineering.

Conclusions

In summary, a high strength, elastic and biocompatible artificial PCL/PU composite vascular graft has been developed with high performance by electrospinning following by pulling out method. After hybrid, the strength of as-prepared PCL/PU scaffold is significantly enhanced up to 69.95 ± 9.12 MPa with the PCL content of 25 wt% and can withstand expansion and contract more than fifteen cycles. The scaffold with the porosity of 70.55 ± 3.24% also demonstrated good cell adhesion and

proliferation. The combination of good and anisotropic mechanical properties, appropriate porosity, cycling stability and cytocompatibility, along with a simple preparation method, make the materials a good replacement for small diameter blood scaffolds and opens the door towards the production of high-performance artificial vascular grafts for tissue engineering.

Acknowledgments

The authors acknowledge the 863 Program (2013AA032203), NSFC (21374001, 21134003, 21433012, 21222309), 973 Program (2012CB933200), Program for New Century Excellent Talents in University of China and the Fundamental Research Funds for the Central Universities.

Notes and references

1 H. G. S. Ayaz, A. Perets, H. Ayaz, K. D. Gilroy, M. Govindaraj, D. Brookstein and P. I. Lelkes. *Biomaterials*, 2014, **35**, 8540-8552.
2 A. Hasan, A. Memic, N. Annabi, M. Hossain, A. Paul, M. R. Dokmeci, F. Dehghani and A. Khademhosseini. *Acta Biomater*, 2014, **10**, 11-25.
3 M. A. Rafiee, J. Rafiee and Z. Wang. *ACS nano* 2009, **3**, 3884-3890.
4 P. Das and A. Walther. *Nanoscale*, 2013, **5**, 9348–9356.
5 S. Deville, E. Saiz, R. K. Nalla and A. P. Tomsia. *Science*, 2006, **311**, 515-518.
6 L. J. Bonderer, A. R. Studart and L. J. Gauckler. *Science*, 2008, **319**, 1069-1073.
7 J. Wang, L. Lin, Q. Cheng and L. Jiang. *Angew. Chem. Int. Ed*., 2012, **51**, 4676-4680.
8 R. Guidoin, N. Chakfé, S. Maurel, T. How, M. Batt, M. Marois and C. Gosselin. *Biomaterials*, 1993, **14**, 678-693.
9 Z. Ma, M. Kotaki and R. Inai. *Tissue Eng.*, 2005,**11**,101-109.
10 D. Li, Y. N. Xia. *Adv.Mater*, 2004, **16**, 1151-1170.
11 W. E. Teo, S. Ramakrishna. *Nanotechnology*, 2006, **17**, R89-R106.
12 Y. Zhao, X. Cao and L. Jiang. *J. Am. Chem. Soc.*, 2007, **129**, 764-765.
13 J. S. Lee, K. Y. Shin, C. Kim and J. Jang. *Chem. Commun*., 2013, **49**, 11047--11049
14 A. Greiner, J. H. Wendorff. *Angew. Chem. Int. Ed*., 2007, **46**, 5670-5703.
15 H. Yang, Y. Lan, W. Zhu, W. Li, D. Xu, J. Cui, D. Shen and G. Li. *J. Mater. Chem.*, 2012, **22**, 16994–17001.
16 J. Wu, N. Wang, Y. Zhao and L. Jiang. *J. Mater. Chem. A*, 2013, **1**, 7290–7305.
17 J. Xie, W. Liu, M. R. MacEwan, P. C. Bridgman, Y. Xia. *ACS nano*, 2014, **8**, 1878-1885.
18 T. J. Sill, H. A. von Recum. *Biomaterials*, 2008, **29**, 1989-2006.
19 C. Huang, S. Wang, L. Qiu, Q. Ke, W. Zhai and X. Mo. *ACS Appl. Mater. Interfaces*, 2013, **5**, 2220-2226.
20 M. Moffa, A. Polini, A. G. Sciancalepore, L. Persano et al. *Soft Matter*, 2013, **9**, 5529-5539
21 Y. M. Ju, J. S. Choi, A. Atala, J. J. Yoo and S. J. Lee. *Biomaterials*, 2010, **31**, 4313-4321.
22 D. Gupta, J. Venugopal, S. Mitra, V. R. Giri Dev and S. Ramakrishna. *Biomaterials*, 2009, **30**, 2085-2094.
23 F. Ahmed, N. K. Dutta, A. Zannettino, K. Vandyke and N. R. Choudhury. *Biomacromolecules*, 2014, **15**, 1276-1287.
24 N. Masoumi, B. L. Larson, N. Annabi, M. Kharaziha, B. Zamanian, K. S. Shapero, A. T. Cubberley, G. Camci-Unal, K. B. Manning, J. E. Mayer and, Jr. A. Khademhosseini. *Adv healthc mater*, 2014, **3**,929-939.
25 Y. Wang, H. Shi, J. Qiao, Y. Tian, M. Wu, W. Zhang, Y. Lin, Z. Niu, and Y. Huang. *ACS Appl. Mater. Interfaces*, 2014, **6**, 2958-2962.
26 D. L. Donovan, S. P. Schmidt, S. P. Townshend, G. O. Njus, and W.V.Sharp. *J Vasc Surg*, 1990, **12**, 531-537.
27 F. Ajalloueian, M. L. Lim, G. Lemon, J. C. Haag, Y. Gustafsson, S. Sjoqvist, A. Beltran-Rodriguez, C. Del Gaudio, S. Baiguera, A. Bianco, P. Jungebluth and P. Macchiarini. *Biomaterials*, 2014, **35**, 5307-5315.
28 M. R. Williamson, R. Black and C. Kielty. *Biomaterials*, 2006, **27**,3608-3616.
29 K. H. Lee, H. Y. Kim, Y. J. Ryu, K. W. Kim and S. W. Choi. *J Polym Sci Part B: Polym Phys*, 2003, **41**, 1256-1262.
30 P. H. S. Picciani, E. S. Medeiros, Z. Pan, D. F. Wood, W. J. Orts, L. H. C. Mattoso and B. G. Soares. *Macromol. Mater. Eng.*, 2010, **295**, 618-627.
31 X. Zhang, R. Nakagawa, K. H. K. Chan and M. Kotaki. *Macromolecules*, 2012, **45**, 5494-5500.
32 I. Dallmeyer, L. T. Lin, Y. Li, F. Ko and J. F. Kadla. *Macromol. Mater. Eng.*, 2014, **299**, 540-551.
33 H. W. Liang, Q. F. Guan, L. F. Chen, Z. Zhu, W. J. Zhang and S. H. Yu. *Angew. Chem. Int. Ed*., 2012, **51**, 5101-5105.
34 L. Persano, C. Dagdeviren, Y. Su, Y. Zhang et al. *Nat. Commun.*, 2013, **4**, 1633-1643
35 M. Z. Seyedin, J. M. Razal, P. C. Innis and G. G. Wallace. *Adv. Func.Mater*, 2014, **24**, 2957-2966.
36 A. Arinstein, M. Burman, O. Gendelman, E. Zussman. *Nat. Nanotech.*, 2007, **2**, 59-62.
37 D. A. Stone, L. S. T. J. Korley. *Macromolecules*, 2010, **43**, 9217–9226
38 C. M. Vaz, S. van Tuijl, C. V. Bouten and F. P. Baaijens. *Acta Biomater*, 2005, **1**, 575-582.